**Title**

Impact of cholesterol and sphingomyelin on intrinsic membrane permeability

**Authors and Affiliations**

Carolin Dahley [a,*], Estella Dora Germaine Garessus [a], Andrea Ebert [a], Kai-Uwe Goss [a,b]

[a] Department of Analytical Environmental Chemistry, Helmholtz Centre for Environmental Research (UFZ), Permoserstraße 15, 04318 Leipzig, Germany

[b] Institute of Chemistry, University of Halle-Wittenberg, Kurt-Mothes-Straße 2, 06120 Halle, Germany

[*] corresponding author

E-mail addresses: carolin.dahley@ufz.de (C. Dahley), estella.garessus@gmx.ch (E.D.G. Garessus), andrea.ebert@ufz.de (A. Ebert), kai-uwe.goss@ufz.de (K.-U. Goss)

**Abstract**

Transwell experiments with Caco-2 or MDCK cells are the gold standard for determining the intestinal permeability of chemicals. The intrinsic membrane permeability ($P_0$), that can be extracted from these experiments, might be comparable to $P_0$ measured in black lipid membrane (BLM) experiments and $P_0$ predicted by the solubility-diffusion model. Unfortunately, the overlap between experimental $P_{0,Caco-2/MDCK}$ and $P_{0,BLM}$ data is very small. So far, differences between both approaches have been attributed to the cholesterol and sphingomyelin content of cell membranes, but the database is too sparse to thoroughly test this theory. To create a diverse dataset, we measured $P_{0,BLM}$ of ten chemicals in BLM experiments using DPhPC and DPhPC/cholesterol/sphingomyelin membranes. The results were compared to predicted BLM data and experimental Caco-2/MDCK data obtained from literature. While $P_{0,BLM}$ of all chemicals was well predicted by the solubility-diffusion model, $P_{0,Caco-2/MDCK}$ was only predictable for rather hydrophilic compounds with logarithmic hexadecane/water partition coefficients below -0.5. The effect of cholesterol and sphingomyelin on $P_{0,BLM}$ was negligibly small.

**Abbreviations**

BLM, black lipid membrane; Caco-2, human colorectal adenocarcinoma cells; Chol, cholesterol; $D_{hex}$, diffusion coefficient in hexadecane; DPhPC, 1,2-diphytanoyl-sn-glycero-3-phosphocholine; $D_w$, diffusion coefficient in water; $f_n$, fraction of the neutral species; $K_{hex/w}$, hexadecane/water partition coefficient; LSER, linear solvent energy relationship; MDCK, Madin-Darby canine kidney cells; $P_0$, intrinsic permeability; $P_{ABL}$, aqueous boundary layer permeability; $P_{app}$, apparent permeability; $P_{cyt}$, cytosol permeability; $P_m$, membrane permeability; SM, sphingomyelin; $x_m$, thickness of membrane hydrocarbon core

**Key words**

passive permeability, black lipid membrane, Caco-2, MDCK, cholesterol, sphingomyelin

## 1. Introduction

Understanding the permeation across cell membranes is a crucial step in predicting the intestinal absorption of chemicals in vivo [1]. The main mechanisms involved in permeation are passive transcellular, passive paracellular and active transport. In this paper, we focus on passive transcellular transport as the most common transportation route in the intestine for all except very hydrophilic molecules [2].

The apparent passive transcellular permeability ($P_{app}$) of a chemical is determined by its apical and basolateral aqueous boundary layer permeability ($P_{ABL}$), apical and basolateral membrane permeability ($P_m$) and cytosol permeability ($P_{cyt}$) [1]:

$$\frac{1}{P_{app}} = \frac{1}{P_{ABL}} + \frac{1}{P_m} + \frac{1}{P_{cyt}} \quad \text{(equation 1)}$$

$P_{ABL}$ and $P_{cyt}$ are independent of the speciation of the chemical, because neutral and ionic species have the same diffusion coefficients in aqueous media. In contrast, according to the pH-partition hypothesis, membranes are not permeable to the ionic species of a chemical. Therefore, $P_m$ is defined by the neutral species and thus dependent on pH [1,3]. For better comparability, the intrinsic permeability ($P_0$), which is independent of pH, was introduced. It can be calculated from $P_m$ and the fraction of the neutral species ($f_n$) at the respective pH [3]:

$$P_0 = \frac{P_m}{f_n} \quad \text{(equation 2)}$$

In vitro, $P_0$ can be determined from transwell experiments with human colorectal adenocarcinoma cells (Caco-2) or Madin-Darby canine kidney cells (MDCK) [1,4]. This method is complex because active and paracellular transport, retention and biotransformation in the cells as well as cytosol and filter permeability have to be taken into account when extracting $P_0$ from experimental data [1]. Black lipid membrane (BLM) experiments, where a well-mixed donor and acceptor chamber are separated by a phospholipid bilayer spanning over an aperture [5], are free of these artefacts [6] and often used as a simplified model for biological membranes [7]. The composition of these artificial membranes is well defined and can be altered systematically, which makes this experimental approach suitable for mechanistic studies.

Although phospholipid bilayers are heterogenous due to the amphiphilic structure of lipids [8], it can be assumed that the inner hydrophobic hydrocarbon core is the limiting barrier for permeation of rather hydrophilic chemicals [6,9]. This hydrocarbon core consists of C16, C18 and other long-chain fatty acids [10] and hexadecane is often used to model its properties due to the comparable chain length [11,12]. Consequently, $P_0$ should be predictable by the simple solubility-diffusion model as a function of the diffusion coefficient in hexadecane ($D_{hex}$), the partition coefficient between hexadecane and water ($K_{hex/w}$) and the thickness of the hydrocarbon core ($x_m$) [13]:

$$P_0 = \frac{D_{hex} * K_{hex/w}}{x_m} \quad \text{(equation 3)}$$

Indeed, a comparison between $P_0$ calculated according to Eq. 3 and $P_0$ derived from BLM experiments has shown good agreement for a diverse set of more than 30 chemicals [6].

Based on these results, it can be hypothesized that the $P_0$ extracted from Caco-2/MDCK experiments might be predictable by both BLM experiments as well as the solubility-diffusion model. Unfortunately, there is almost no overlap between published Caco-2/MDCK and BLM data. Lomize and Pogozheva [9] identified only five organic chemicals where experimental values are available for both systems. To expand the dataset, they also included six experimental liposome permeabilities in the comparison. All

permeabilities were higher in BLM and liposome experiments than in cell experiments. The authors hypothesized that this discrepancy could be explained by the different lipid composition of artificial and biological membranes. They mentioned especially cholesterol and sphingomyelin because cholesterol is known for increasing the order and thickness of phospholipid membranes, thereby decreasing the permeability [14].

Therefore, the aims of this study were to: (i) examine the influence of physiological amounts of cholesterol and sphingomyelin on BLM permeability, (ii) create an overlap between BLM data and existing Caco-2/MDCK data and (iii) compare predicted and experimental BLM data with Caco-2/MDCK data.

## 2. Material and methods

### *2.1. BLM experiments*

#### *2.1.1. Selection of test compounds*

The test compounds were selected based on a review of $P_0$ extracted from MDCK/Caco-2 experiments [1]. Zwitterions were excluded, because the permeability of zwitterions might be substantially lower than the permeability of the neutral species as studies with amino acids indicated [15]. Furthermore, we excluded chemicals for which active transport might have affected the calculation of $P_{0,Caco\text{-}2/MDCK}$. Eleven chemicals were selected based on their diversity in $P_{0,Caco\text{-}2/MDCK}$ and predicted $P_{0,BLM}$, sufficient water solubility and detectability via LC-MS. One of these chemicals, cimetidine, was subsequently excluded due to effects on membrane integrity (see Supplementary data for details). All selected chemicals are listed in Table S1 in the Supplementary data. Salicylic acid was chosen to validate the system, because both BLM and Caco-2/MDCK data are published for this compound.

#### *2.1.2. Selection of membrane lipids*

1,2-diphytanoyl-sn-glycero-3-phosphocholine (DPhPC) was used for membrane formation due to its high stability [16] and permanent liquid crystalline state at room temperature [17]. To create membranes with a more physiological composition, we also used a mix of 58 mol% DPhPC, 36 mol% cholesterol (Chol) and 6 mol% sphingomyelin (SM) based on a publication by Symons et al. on the lipid composition of MDCK plasma membranes [18].

#### *2.1.3. Selection of experimental pH*

We selected a suitable pH based on the permeability measured in Caco-2/MDCK experiments and predicted by the solubility-diffusion model. In preliminary experiments, we determined a log $P_{ABL}$ of about -3.6, which corresponds to a total ABL thickness of about 250 µm. To assure that the effect of the ABL is negligible, log $P_{app,BLM}$ of the test compound at the chosen pH had to be about -4.1 or lower. Reducing the $f_n$ by adapting the buffer pH allowed us to adjust $P_{app,BLM}$ in accordance with Eq. 2. Limited by the instability of the membrane at extreme pH, we used the following buffers between pH 4 and 10: 10 mM β-alanine (pH 4), 5 mM β-alanine and 5 mM MES (pH 5), 10 mM MES (pH 6), 10 mM MOPS (pH 7), 10 mM TAPS (pH 8 and pH 9) and 10 mM CAPSO (pH 10). All buffer solutions contained 1 mM KCl buffer for electrical measurement of membrane capacitance.

#### *2.1.4. Measurement*

The experiments were conducted at room temperature (20-27 °C). The experimental setup consisted of a Delrin bilayer chamber and a polystyrene cup (diameter: 13 mm) with a customized aperture (diameter: 1 mm) (Multi Channel Systems MCS GmbH a division of Harvard Bioscience, Inc., Reutlingen,

Germany). The aperture was pre-painted with DPhPC (total lipid concentration: 20 µg/µl) or DPhPC/Chol/SM mix (total lipid concentration: 28 µg/µl) dissolved in decane to create a hydrophobic anchor. A higher total lipid concentration was used in the DPhPC/Chol/SM mix because no stable membrane could be formed with less lipid. The assembled chamber was placed on a Cimarec i Mono Direct Stirrer (Thermo Fisher Scientific Inc., Waltham, USA) set to about 400 rpm. 1 ml buffer solution was added to each compartment. Ag/AgCl electrodes were placed in each compartment and an eONE single channel amplifier and the corresponding software Elements Data Reader version 3.7.14 and 3.8.3 were used (Elements SRL, Cesena, Italy) for electrical measurements. Membranes were painted according to Mueller et al. [19,20] using the same lipid composition as for pre-painting. Specific capacitance values between 0.3 and 0.6 µF/cm² indicated the formation of a membrane. During electrical measurements, a faraday cage was placed on top of the chamber to reduce noise. After 30 min, 50 µl buffer was removed from both sides and analysed for possible contaminations. The volume was replaced with fresh buffer. 100-200 µl buffer was removed from the donor chamber and replaced with the stock solution of the chemical of interest. We aimed to keep the concentration on the donor side as low as possible to avoid effects of the test compound on membrane integrity, but sufficiently high to be still detectable on the acceptor side. 50 µl samples from the acceptor side were taken after 15 min, 1 h and then every hour until the membrane collapsed or the capacitance was outside the predefined range. Due to instability at pH 10, the samples were taken after 15 min, 1 h and then every 30 min. The removed sample volume was replaced with fresh buffer each time. All experiments were performed at least in duplicate.

*2.1.5. Sample analysis*

Sample analysis was conducted using an Infinity II 1260 LC system coupled to a 6420 triple quadrupole with ESI source (Agilent Technologies Inc., Santa Clara, USA). Depending on the peak shape and area either Kinetex® F5 (2.6 µm; 100 Å; 50 * 3.0 mm) or Kinetex® C18 (2.6 µm; 100 Å; 50 * 3.0 mm) LC columns were used (Phenomenex Inc., Torrance, USA). The columns were protected by KrudKatcher™ ULTRA HPLC In-Line Filters and SecurityGuard™ ULTRA Catridges (Phenomenex Inc., Torrance, USA). Double distilled water with 5 mM ammonium acetate and 1 % MeOH (pH 7.3) or double distilled water with 1 % MeOH and 0.1 % HCOOH (pH 2.7) was used as eluent A, while MeOH with 0.1 % HCOOH was used as eluent B.

*2.1.6. Data analysis*

$P_{app,BLM}$ for each time interval was calculated as follows:

$$P_{app,BLM} = \frac{c_{tx} - c_{tx-1} * 0.95}{t_x - t_{x-1}} * \frac{V}{A * \Delta c} \quad \text{(equation 4)}$$

Where $c_{tx}$ and $c_{tx-1}$ are the acceptor concentrations measured at the two consecutive time points $t_x$ and $t_{x-1}$. A dilution correction factor of 0.95 accounts for the removal of 50 µl acceptor volume and the replacement with fresh buffer during sampling. V is the volume of the acceptor chamber, A is the membrane area and Δc is the applied concentration difference. $P_{app,BLM}$ from each time interval and replicate were averaged to obtain the mean $P_{app,BLM}$ and the associated standard deviation.

Given that $P_{cyt}$ is non-existent in BLM experiments and the impact of $P_{ABL}$ is negligible at the selected buffer pH, $P_{app,BLM}$ was equated to $P_m$ and $P_{0,BLM}$ was calculated according to Eq. 2. $f_n$ was calculated based on the experimental $pK_{a\,(25\,°C)}$ provided by Avdeef [1] (see Eq. S1 in the Supplementary data) and checked for plausibility with JChem for Office [21]. If no experimental $pK_{a\,(25\,°C)}$ was available, it was recalculated from $pK_{a\,(37\,°C)}$ as described elsewhere [22].

166 *2.2. Prediction of $P_{0,LSER}$ by the solubility-diffusion model*

167 $P_{0,LSER}$ was calculated according to Eq. 3. $D_{hex\ (25\ °C)}$ was assumed to be one tenth of the diffusion
168 coefficient in water ($D_{w\ (25\ °C)}$). [6] $D_{w\ (25\ °C)}$ was estimated from the molecular weight (MW) of the
169 compound [23]:

170 $$D_{hex} = 0.1 * 10^{(-4.13-0.453*\log(MW))} \quad \text{(equation 5)}$$

171 Based on experimental Linear Solvation Energy Relationship (LSER) descriptors, $K_{hex/w\ (25\ °C)}$ was
172 predicted using UFZ-LSER database [24] (see Table S2 in the Supplementary data). Experimental
173 descriptors were taken from "UFZ-preselected published values" dataset if available. Otherwise, the
174 "Abraham Absolv" dataset was used. The hydrocarbon core thickness $x_m$ was estimated from the
175 specific capacitance ($C_m$) using the vacuum permittivity ($\varepsilon_0$) of 8.85 * $10^{-12}$ F/m and the dielectric
176 constant of the hydrocarbon core ($\varepsilon_m$) of 2.1 [16,25]:

177 $$x_m = \frac{\varepsilon_0 * \varepsilon_m}{C_m} \quad \text{(equation 6)}$$

178 For $C_m$ between 0.3 and 0.6 µF/cm² this results in a $x_m$ of about 40 Å.

179 *2.3. Comparison of BLM and LSER data with Caco-2/MDCK data*

180 To compare $P_{0,BLM}$ and $P_{0,LSER}$ at 25 °C with $P_{0,Caco\text{-}2/MDCK}$ at 37 °C, adjustments were necessary. A
181 temperature correction factor of 1.348 was included in the calculation of $D_{hex}$ [4]. $P_{0,BLM}$ and $P_{0,LSER}$ were
182 multiplied by 2 because cell membranes with 20 Å [25] are only half as thick as BLM formed with
183 decane as solvent. The presence of two (apical and basolateral) membranes in cell experiments was
184 considered by adding their resistances and a correction factor of 24 was included in the calculation of
185 the permeability of the apical membrane to take into account that the surface area is increased by
186 microvilli [6,26]:

187 $$P_{0^*\ (37\ °C)} = \frac{1}{R_{apical} + R_{basolateral}} = \frac{1}{\frac{1}{P_{0\ (25\ °C)} * 1.348 * 2 * 24} + \frac{1}{P_{0\ (25\ °C)} * 1.348 * 2}} \quad \text{(equation 7)}$$

188

189 **3. Results and Discussion**

190 *3.1. Prediction of log $P_{0,BLM}$ by the solubility-diffusion model*

191 $P_{app,BLM}$ of ten chemicals was determined in BLM experiments. The resulting log $P_{0,BLM}$ values cover six
192 orders of magnitude. Log $P_{0,BLM}$ of salicylic acid was measured to validate the system because BLM data
193 from literature are available for this compound. With log $P_{0,BLM}$ [P in cm/s] of -0.13, our result is in good
194 agreement with the reported values of 0.08 [27], -0.11 [28,29] and -0.15 [30], although different lipids
195 and membrane forming techniques are used. While Gutknecht [28], Gutknecht and Tosteson [30] and
196 Walter and Gutknecht [29] used egg lecithin and the painting technique, Saparov et al. [27] used DPhPC
197 and the folding technique [31]. The comparable results suggests that log $P_{0,BLM}$ of pure lipid membranes
198 is not significantly affected by the used lipid or technique. This assumption is supported by a study by
199 Walter and Gutknecht [29] who also reported negligible differences between used lipids and
200 techniques for three organic acids.

201 To verify the hypothesis that log $P_{0,BLM}$ should be predictable by the solubility-diffusion model, log $P_{0,LSER}$
202 values predicted with Eq. 3 are compared to experimental log $P_{0,BLM}$ values in Fig. 1. For all compounds
203 the deviation between both values is within about one order of magnitude. This range was expected
204 given the uncertainty associated with estimating $K_{hex/w}$ from experimental LSER descriptors with

varying quality. It supports the work of Bittermann and Goss [6] who also found good agreement between experimental log $P_{0,BLM}$ and predicted log $P_{0,LSER}$ of 37 compounds.

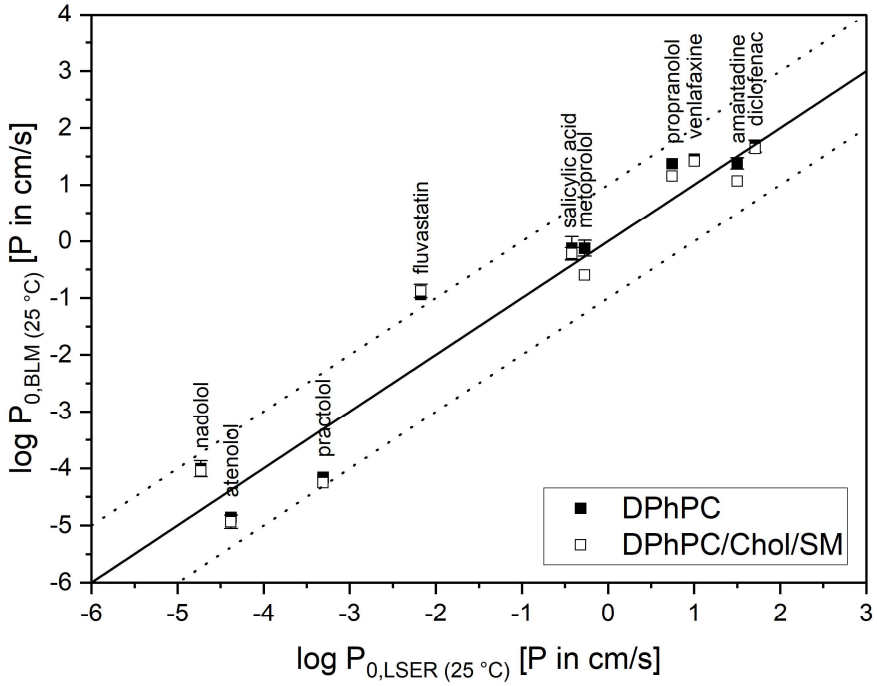


Figure 1: Comparison of predicted log $P_{0,LSER}$ and experimental log $P_{0,BLM}$ derived from pure DPhPC and DPhPC/Chol/SM membranes. Symbols represent the average log $P_{0,BLM}$ of two to three replicates +/- standard deviation. Error bars are only shown when they exceed the size of the symbol. All values are listed in Table S3 in the Supplementary data.

### *3.2. Difference between pure DPhPC and DPhPC/Chol/SM membranes*

To examine the effect of Chol and SM on BLM permeability, log $P_{0,BLM}$ was determined for both pure DPhPC membranes and DPhPC membranes containing physiological amounts of Chol and SM. As shown in Fig. 1, log $P_{0,BLM}$ of pure DPhPC membranes is slightly higher than log $P_{0,BLM}$ of DPhPC/Chol/SM membranes for all compounds except fluvastatin. Nevertheless, with 0.14 log units on average, the difference in log $P_{0,BLM}$ between both membrane types is mostly within the observed standard deviation and could be attributed to measurement uncertainties. More significant differences were reported by Finkelstein who compared the permeability of pure lecithin membranes and lecithin membranes containing 67 % cholesterol and found differences of 0.6 up to 1.1 log units for four organic compounds [12]. Xiang et al. got a similar difference of 0.6 log units when comparing the permeability of two compounds across lecithin membranes with and without 30 mol% cholesterol [32]. This permeability decreasing effect of cholesterol is attributed to the ordering effect on acyl chains [33] as well as the condensing effect that reduces the surface area per lipid molecule and therefore increases the membrane thickness [14,33]. A possible reason for the smaller impact of cholesterol on our membranes is the usage of DPhPC instead of lecithin. The methylated acyl chains of DPhPC may impede the ordering effect of cholesterol by steric hindrance [34]. It may be also possible that the coexistence of SM reduces the ordering effect of cholesterol. This hypothesis is supported by a study by van Duyl et al. [35] who examined the influence of SM on cholesterol-containing DOPC membranes. They found that SM-containing membranes are less ordered by cholesterol and attributed this to the high affinity of Chol to SM, resulting in the formation of Chol/SM rich domains at ambient temperature. This implies

that less Chol is located in the glycerophospholipid part of the membrane and the ordering effect is reduced.

### *3.3. Comparison of predicted log $P_{0,LSER*}$ and experimental log $P_{0,BLM*}$ and log $P_{0,Caco-2/MDCK}$*

For comparison with log $P_{0,Caco-2/MDCK}$ obtained from literature [1], we did not adjust the prediction of log $P_{0,LSER}$ to the Chol and SM content of cell membranes, because the effect seems to be negligible. But nevertheless we used log $P_{0,BLM}$ derived from experiments with DPhPC/Chol/SM membranes due to the higher similarity to cell membranes. Log $P_{0,BLM}$ as well as log $P_{0,LSER}$ were adjusted for differences in temperature, surface area, number and thickness of membranes according to Eq. 7. The resulting log $P_{0,BLM*}$ and log $P_{0,LSER*}$ are plotted against log $P_{0,Caco-2/MDCK}$ in Fig 2. For five compounds all three datasets are in good accordance, but there are substantial differences for the five remaining compounds. Therefore, our results do not support the hypothesis by Lomize and Pogozheva [9] that the differences between log $P_{0,BLM}$ and log $P_{0,Caco-2/MDCK}$ are caused by the Chol and SM content of cell membranes. Even differences of about 0.6 log units between the permeability of cholesterol-containing and cholesterol-free membranes as described by Finkelstein [12] and Xiang et al. [32] could not explain these discrepancies of up to 4.7 log units. Instead, prevailing differences seem to be related to log $K_{hex/w}$. The five compounds in our dataset, where log $P_{0,BLM*}$, log $P_{0,LSER*}$ and log $P_{0,Caco-2/MDCK}$ are in good accordance, are those with low log $K_{hex/w}$ (log $K_{hex/w}$ = -4.87 to -0.72). Neglecting liposome permeabilities, the five organic compounds included in Lomize and Pogozheva's [9] comparison of experimental log $P_{0,BLM}$ and log $P_{0,Caco-2/MDCK}$ also have low log $K_{hex/w}$ (log $K_{hex/w}$ = -7 to -0,72). The maximum deviation between both values in their dataset does not exceed 1.3 log units, which supports our assumption that BLM experiments can be used to predict log $P_{0,Caco-2/MDCK}$ of hydrophilic compounds. The five deviating compounds in our dataset are those with high log $K_{hex/w}$ which implicates that the prediction of experimental log $P_{0,Caco-2/MDCK}$ is problematic for rather lipophilic compounds. Based on the solubility-diffusion theory, log $P_{0,Caco-2/MDCK}$ should increase with increasing log $K_{hex/w}$. It is therefore contrary to mechanistic understanding that compounds with high log $K_{hex/w}$ as metoprolol, propranolol, venlafaxine, amantadine and diclofenac (log $K_{hex/w}$ = -0,44 to 1,56) permeate slower through cell membranes than compounds with smaller log $K_{hex/w}$ such as salicylic acid (log $K_{hex/w}$ = -0,72). A possible explanation is the limiting effect of the ABL. Rather lipophilic compounds may find their main resistance in the ABL instead of the membrane leading to inaccurate calculations of log $P_{0,Caco-2/MDCK}$. Nevertheless, this explanation seems unlikely because Avdeef took great care to eliminate the effects of the ABL in his data collection [1]. Another possible reason is that biological membranes consist of more than phospholipids, cholesterol and sphingomyelin. Membrane proteins might reduce the passive permeability of chemicals by reducing the accessible membrane surface area or increasing the membrane thickness [36]. But these effects should decrease the permeability of all molecules, not only lipophilic ones. Apart from differences in the composition of artificial and biological membranes, it must also be considered that effects in the cytosol could be responsible for the deviation of rather lipophilic compounds. This will be the main focus of our future research.

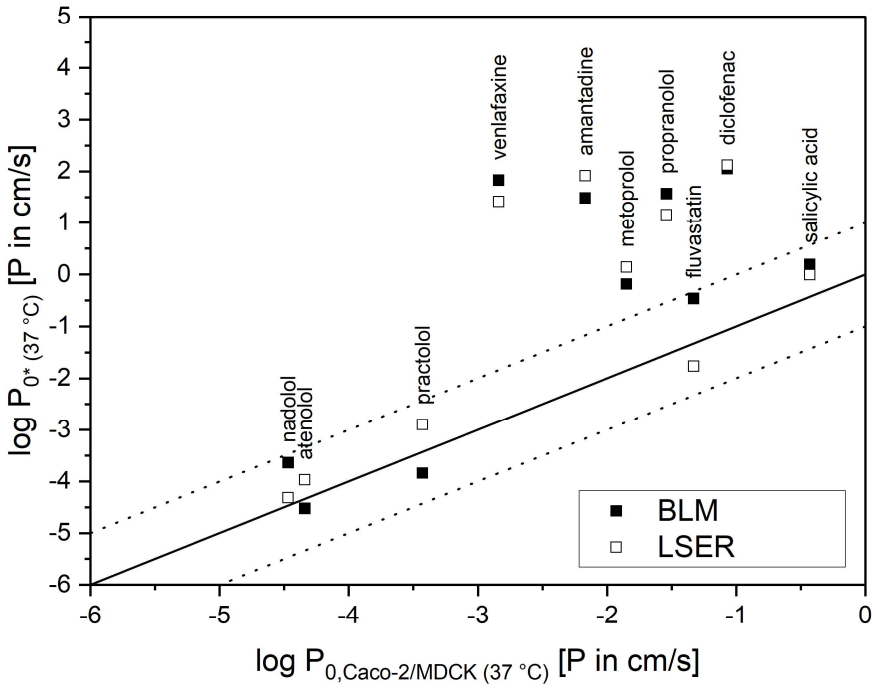


Figure 2: Comparison of predicted log $P_{0,LSER*}$, experimental log $P_{0,BLM*}$ and experimental log $P_{0,Caco-2/MDCK}$. Log $P_{0,LSER*}$ and log $P_{0,BLM*}$ were calculated from respective log $P_{0,LSER}$ and log $P_{0,BLM}$ derived from DPhPC/Chol/SM membranes and adjusted for temperature, surface area, number and thickness of membranes. All values are listed in Table S3 in the Supplementary data.

## 4. Conclusion

Log $P_{0,BLM}$ is well predicted by the solubility-diffusion model using LSER, especially when high-quality experimental descriptors are available. The influence of Chol and SM on log $P_{0,BLM}$ seems to be minimal. Nevertheless, using experimental log $P_{0,BLM}$ as well as predicted log $P_{0,LSER}$ to predict log $P_{0,Caco-2/MDCK}$ remains problematic. While compounds with log $K_{hex/w}$ values below -0.5 seem to be well predicted, compounds with higher log $K_{hex/w}$ values show unexpectedly low log $P_{0,Caco-2/MDCK}$. This deviation of rather lipophilic compounds has to be addressed in future research.

## Appendix A. Supplementary data

## References

[1] A. Avdeef, Absorption and drug development. Solubility, permeability, and charge state, 2nd ed., John Wiley & Sons, Hoboken N.J., 2012.

[2] P. Artursson, K. Palm, K. Luthman, Caco-2 monolayers in experimental and theoretical predictions of drug transport, Adv. Drug Deliver. Rev. 64 (2012) 280–289. https://doi.org/10.1016/j.addr.2012.09.005.

[3] A. Avdeef, Physicochemical profiling (solubility, permeability and charge state), Curr. Top. Med. Chem. 1 (2001) 277–351. https://doi.org/10.2174/1568026013395100.

[4] A. Avdeef, P. Artursson, S. Neuhoff, L. Lazorova, J. Gråsjö, S. Tavelin, Caco-2 permeability of weakly basic drugs predicted with the double-sink PAMPA pKa(flux) method, Eur. J. Pharm. Sci. 24 (2005) 333–349. https://doi.org/10.1016/j.ejps.2004.11.011.
[5] P. Mueller, D.O. Rudin, H.T. Tien, W.C. Wescott, Reconstitution of cell membrane structure in vitro and its transformation into an excitable system, Nature 194 (1962) 979–980. https://doi.org/10.1038/194979a0.
[6] K. Bittermann, K.-U. Goss, Predicting apparent passive permeability of Caco-2 and MDCK cell-monolayers: A mechanistic model, PLoS ONE 12 (2017) e0190319. https://doi.org/10.1371/journal.pone.0190319.
[7] Š. Skalová, V. Vyskočil, J. Barek, T. Navrátil, Model Biological Membranes and Possibilities of Application of Electrochemical Impedance Spectroscopy for their Characterization, Electroanalysis 30 (2018) 207–219. https://doi.org/10.1002/elan.201700649.
[8] C. Hannesschlaeger, A. Horner, P. Pohl, Intrinsic Membrane Permeability to Small Molecules, Chem. Rev. 119 (2019) 5922–5953. https://doi.org/10.1021/acs.chemrev.8b00560.
[9] A.L. Lomize, I.D. Pogozheva, Physics-Based Method for Modeling Passive Membrane Permeability and Translocation Pathways of Bioactive Molecules, J. Chem. Inf. Model. 59 (2019) 3198–3213. https://doi.org/10.1021/acs.jcim.9b00224.
[10] G. Enkavi, M. Javanainen, W. Kulig, T. Róg, I. Vattulainen, Multiscale Simulations of Biological Membranes: The Challenge To Understand Biological Phenomena in a Living Substance, Chem. Rev. 119 (2019) 5607–5774. https://doi.org/10.1021/acs.chemrev.8b00538.
[11] A. Walter, J. Gutknecht, Permeability of small nonelectrolytes through lipid bilayer membranes, J. Membr. Biol. 90 (1986) 207–217. https://doi.org/10.1007/BF01870127.
[12] A. Finkelstein, Water and nonelectrolyte permeability of lipid bilayer membranes, J. Gen. Physiol. 68 (1976) 127–135. https://doi.org/10.1085/jgp.68.2.127.
[13] A. Missner, P. Pohl, 110 years of the Meyer-Overton rule: predicting membrane permeability of gases and other small compounds, Chemphyschem 10 (2009) 1405–1414. https://doi.org/10.1002/cphc.200900270.
[14] F. de Meyer, B. Smit, Effect of cholesterol on the structure of a phospholipid bilayer, Proc. Natl. Acad. Sci. USA 106 (2009) 3654–3658. https://doi.org/10.1073/pnas.0809959106.
[15] A.C. Chakrabarti, D.W. Deamer, Permeability of lipid bilayers to amino acids and phosphate, Biochim. Biophys. Acta Biomembr. 1111 (1992) 171–177. https://doi.org/10.1016/0005-2736(92)90308-9.
[16] T. Baba, Y. Toshima, H. Minamikawa, M. Hato, K. Suzuki, N. Kamo, Formation and characterization of planar lipid bilayer membranes from synthetic phytanyl-chained glycolipids, Biochim. Biophys. Acta Biomembr. 1421 (1999) 91–102. https://doi.org/10.1016/S0005-2736(99)00114-5.
[17] H. Lindsey, N.O. Petersen, S.I. Chan, Physicochemical characterization of 1,2-diphytanoyl-sn-glycero-3-phosphocholine in model membrane systems, Biochim. Biophys. Acta Biomembr. 555 (1979) 147–167. https://doi.org/10.1016/0005-2736(79)90079-8.
[18] J.L. Symons, K.-J. Cho, J.T. Chang, G. Du, M.N. Waxham, J.F. Hancock, I. Levental, K.R. Levental, Lipidomic atlas of mammalian cell membranes reveals hierarchical variation induced by culture conditions, subcellular membranes, and cell lineages, Soft Matter 17 (2021) 288–297. https://doi.org/10.1039/d0sm00404a.
[19] P. Mueller, D.O. Rudin, H.T. Tien, W.C. Wescott, Methods for the Formation of Single Bimolecular Lipid Membranes in Aqueous Solution, J. Phys. Chem. 67 (1963) 534–535. https://doi.org/10.1021/j100796a529.

[20] T. Gutsmann, T. Heimburg, U. Keyser, K.R. Mahendran, M. Winterhalter, Protein reconstitution into freestanding planar lipid membranes for electrophysiological characterization, Nat. Protoc. 10 (2015) 188–198. https://doi.org/10.1038/nprot.2015.003.
[21] ChemAxon, JChem for Office v21.3.0.817 (2021). http://www.chemaxon.com.
[22] N. Sun, A. Avdeef, Biorelevant pK(a) (37 °C) predicted from the 2D structure of the molecule and its pK(a) at 25 °C, J. Pharmaceut. Biomed. 56 (2011) 173–182. https://doi.org/10.1016/j.jpba.2011.05.007.
[23] A. Avdeef, Leakiness and size exclusion of paracellular channels in cultured epithelial cell monolayers-interlaboratory comparison, Pharm. Res. 27 (2010) 480–489. https://doi.org/10.1007/s11095-009-0036-7.
[24] N. Ulrich, S. Endo, T.N. Brown, N. Watanabe, G. Bronner, M.H. Abraham, K.-U. Goss, UFZ-LSER database v3.2.1 (2017). http://www.ufz.de/lserd.
[25] R. Fettiplace, D.M. Andrews, D.A. Haydon, The thickness, composition and structure of some lipid bilayers and natural membranes, J. Membr. Biol. 5 (1971) 277–296. https://doi.org/10.1007/BF01870555.
[26] S.L. Palay, L.J. Karlin, An Electron Microscopic Study of the Intestinal Villus: II. The Pathway of Fat Absorption, J. Biophys. Biochem. Cytol. 5 (1959) 373–384. https://doi.org/10.1083/jcb.5.3.373.
[27] S.M. Saparov, Y.N. Antonenko, P. Pohl, A new model of weak acid permeation through membranes revisited: does Overton still rule?, Biophys. J. 90 (2006) L86-8. https://doi.org/10.1529/biophysj.106.084343.
[28] J. Gutknecht, Aspirin, acetaminophen and proton transport through phospholipid bilayers and mitochondrial membranes, Mol. Cell. Biochem. 114 (1992) 3–8. https://doi.org/10.1007/BF00240290.
[29] A. Walter, J. Gutknecht, Monocarboxylic acid permeation through lipid bilayer membranes, J. Membr. Biol. 77 (1984) 255–264. https://doi.org/10.1007/BF01870573.
[30] J. Gutknecht, D.C. Tosteson, Diffusion of weak acids across lipid bilayer membranes: effects of chemical reactions in the unstirred layers, Science 182 (1973) 1258–1261. https://doi.org/10.1126/science.182.4118.1258.
[31] M. Montal, P. Mueller, Formation of bimolecular membranes from lipid monolayers and a study of their electrical properties, Proc. Natl. Acad. Sci. USA 69 (1972) 3561–3566. https://doi.org/10.1073/pnas.69.12.3561.
[32] T.X. Xiang, J. Chen, B.D. Anderson, A quantitative model for the dependence of solute permeability on peptide and cholesterol content in biomembranes, J. Membr. Biol. 177 (2000) 137–148. https://doi.org/10.1007/s002320001107.
[33] T. Róg, M. Pasenkiewicz-Gierula, I. Vattulainen, M. Karttunen, Ordering effects of cholesterol and its analogues, Biochim. Biophys. Acta 1788 (2009) 97–121. https://doi.org/10.1016/j.bbamem.2008.08.022.
[34] W.C. Hung, F.Y. Chen, H.W. Huang, Order–disorder transition in bilayers of diphytanoyl phosphatidylcholine, Biochim. Biophys. Acta Biomembr. 1467 (2000) 198–206. https://doi.org/10.1016/S0005-2736(00)00221-2.
[35] B.Y. van Duyl, D. Ganchev, V. Chupin, B. de Kruijff, J. Killian, Sphingomyelin is much more effective than saturated phosphatidylcholine in excluding unsaturated phosphatidylcholine from domains formed with cholesterol, FEBS Lett. 547 (2003) 101–106. https://doi.org/10.1016/S0014-5793(03)00678-1.
[36] K. Mitra, I. Ubarretxena-Belandia, T. Taguchi, G. Warren, D.M. Engelman, Modulation of the bilayer thickness of exocytic pathway membranes by membrane proteins rather than

386 cholesterol, Proc. Natl. Acad. Sci. USA 101 (2004) 4083–4088.
387 https://doi.org/10.1073/pnas.0307332101.